



## FXR agonist activity of conformationally constrained analogs of GW 4064

Adwoa Akwabi-Ameyaw<sup>a,†</sup>, Jonathan Y. Bass<sup>a,‡</sup>, Richard D. Caldwell<sup>a,§</sup>, Justin A. Caravella<sup>b,¶</sup>, Lihong Chen<sup>c</sup>, Katrina L. Creech<sup>d</sup>, David N. Deaton<sup>a</sup>, Kevin P. Madauss<sup>b</sup>, Harry B. Marr<sup>e</sup>, Robert B. McFadyen<sup>a</sup>, Aaron B. Miller<sup>b</sup>, Frank Navas III<sup>a,\*</sup>, Derek J. Parks<sup>f</sup>, Paul K. Spearing<sup>a</sup>, Dan Todd<sup>g</sup>, Shawn P. Williams<sup>b</sup>, G. Bruce Wisely<sup>f</sup>

<sup>a</sup> Department of Medicinal Chemistry, GlaxoSmithKline, Research Triangle Park, NC 27709, USA

<sup>b</sup> Molecular Discovery Research, Computational and Structural Chemistry Research, GlaxoSmithKline, Research Triangle Park, NC 27709, USA

<sup>c</sup> Department of Metabolic Diseases, GlaxoSmithKline, Research Triangle Park, NC 27709, USA

<sup>d</sup> Molecular Discovery Research, Screening & Compound Profiling, GlaxoSmithKline, Research Triangle Park, NC 27709, USA

<sup>e</sup> Department of Drug Metabolism and Pharmacokinetics, GlaxoSmithKline, Research Triangle Park, NC 27709, USA

<sup>f</sup> Molecular Discovery Research, Biological Reagents and Assay Development, GlaxoSmithKline, Research Triangle Park, NC 27709, USA

<sup>g</sup> Department of Pharmaceutical Development, Physical Properties and Developability, GlaxoSmithKline, Research Triangle Park, NC 27709, USA

### ARTICLE INFO

#### Article history:

Received 12 May 2009

Revised 12 June 2009

Accepted 15 June 2009

Available online 21 June 2009

#### Keywords:

Farnesoid X receptor

FXR

Nuclear receptor

### ABSTRACT

Two series of conformationally constrained analogs of the FXR agonist GW 4064 **1** were prepared. Replacement of the metabolically labile stilbene with either benzothiophene or naphthalene rings led to the identification of potent full agonists **2a** and **2g**.

© 2009 Elsevier Ltd. All rights reserved.

The farnesoid X receptor (FXR) is a human nuclear receptor that is expressed in a variety of tissues including liver, gall bladder, intestines, kidney, and adrenal gland.<sup>1,2</sup> Activation of FXR by its natural ligands, bile acids, influences a variety of biochemical processes through gene transcription, including bile acid<sup>3,4</sup> and glucose homeostasis,<sup>5–7</sup> lipid regulation,<sup>8–10</sup> and control of bacterial growth in the intestines.<sup>11–13</sup> The many physiological roles played by this nuclear receptor suggests that FXR modulators may be useful in treating a wide range of diseases, including diabetes,<sup>7</sup> cholestasis,<sup>14–16</sup> liver fibrosis,<sup>17–19</sup> atherosclerosis,<sup>20,21</sup> and inflammatory bowel disease.<sup>11,12</sup>

GlaxoWellcome scientists have reported the discovery of a potent FXR agonist, GW 4064 **1**, which has been utilized by numerous investigators to reveal the biological functions of FXR.<sup>9</sup> While GW

4064 **1** is a useful tool compound, it has issues that complicate its further development. These liabilities include, poor pharmacokinetics in the rat ( $t_{1/2} < 1$  h,  $C_l = 36$  mL/min/kg,  $F < 10\%$ ),<sup>22,23</sup> a potentially toxic stilbene pharmacophore,<sup>24,25</sup> and stilbene-mediated UV light instability.<sup>22</sup> In an attempt to address the various liabilities of its stilbene functional group, GSK researchers prepared a series of conformationally constrained naphthoic acid analogs.<sup>22</sup> Through this effort, a potent FXR agonist GSK8062 was identified, which exhibited improved developability parameters and was efficacious in the ANIT rat model of cholestasis. Herein, these researchers describe two new series of conformationally constrained analogs of **1**, wherein the central aromatic ring is linked either to the distal stilbene carbon or the proximal stilbene carbon as exemplified by structures **2a** and **3a**, respectively. As in GW 4064 **1**, the compounds in series **2** and **3** contain a similar atom count between the isoxazole and benzoic acid rings. A key difference, however, is that the connectors in series **2** contain one less rotatable bond than series **3** or GW 4064 **1**. The additional conformational constraint in series **2** may provide a boost in potency. In both series, the newly formed bicyclic rings include 5–6, 6–6, and 6–5 ring systems. Since the *meta*-carboxylic acid may not be optimal for activity in these series, the *para*-isomers of selected compounds were also prepared.

\* Corresponding author at present address: 609 Churchill Drive, Chapel Hill, NC 27517, USA. Tel.: +1 919 968 9181.

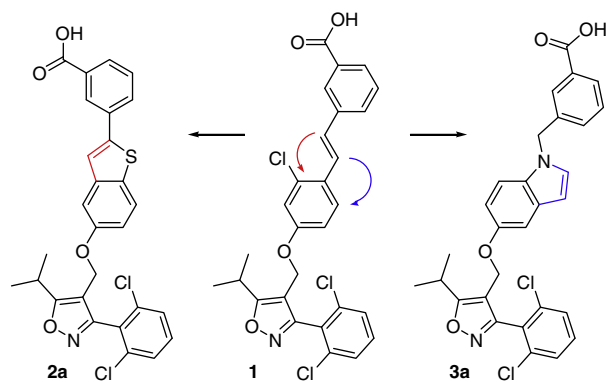
E-mail address: [frank.navas3@gmail.com](mailto:frank.navas3@gmail.com) (F. Navas III).

† Present address: 409 Sir Walker Lane, Cary, NC 27519, USA.

‡ Present address: Department of Chemistry, University of California, Irvine, CA 92697, USA.

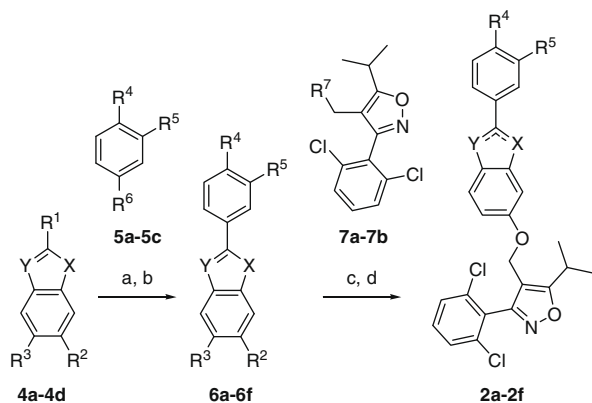
§ Present address: Biogen Idec, 14 Cambridge Center, Cambridge, MA 02142, USA.

¶ Present address: Biogen Idec, 14 Cambridge Center, Cambridge, MA 02142, USA.

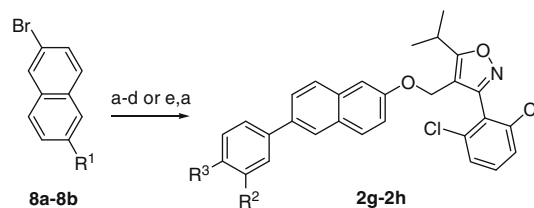


The preparation of compounds **2a–f** is depicted in **Scheme 1**.<sup>26</sup> The commercially available 5-methoxybenzothiophene-2-boronic acid **4a** ( $R^1 = B(OH)_2$ ,  $R^2 = H$ ,  $R^3 = OMe$ ,  $X = S$ ,  $Y = CH$ ) and 6-methoxybenzothiophene-2-boronic acid **4b** ( $R^1 = B(OH)_2$ ,  $R^2 = OMe$ ,  $R^3 = H$ ,  $X = S$ ,  $Y = CH$ ) were coupled to ethyl 3-iodobenzoate **5a** ( $R^4 = H$ ,  $R^5 = COOEt$ ,  $R^6 = I$ ) and ethyl 4-iodobenzoate **5b** ( $R^4 = COOEt$ ,  $R^5 = H$ ,  $R^6 = I$ ), employing the Suzuki protocol, then the methyl aryl ethers were cleaved with boron tribromide to provide the phenols **6a–d**. The phenol **6e** was synthesized in a similar manner from 2-bromo-6-methoxybenzothiazole **4c** ( $R^1 = Br$ ,  $R^2 = OMe$ ,  $R^3 = H$ ,  $X = S$ ,  $Y = N$ ) and 3-methoxycarbonylphenylboronic acid **5c** ( $R^4 = H$ ,  $R^5 = COOMe$ ,  $R^6 = B(OH)_2$ ). The phenol **6f** was synthesized via Suzuki coupling of 1-*tert*-butyloxycarbonyl-5-benzyloxy-indole-2-boronic acid **4d** ( $R^1 = B(OH)_2$ ,  $R^2 = OBn$ ,  $R^3 = H$ ,  $X = CH$ ,  $Y = NCOOC(CH_3)_3$ ) and ethyl 3-iodobenzoate **5a**, followed by hydrogenolysis of the benzyl ether protecting group. The phenols **6a–f** were then alkylated with the known alcohol **7a** ( $R^7 = OH$ ) under Mitsunobu conditions, followed by hydrolysis of the esters (and the *tert*-butylcarbamate of **2f**) to afford the acids **2a–f**.

The naphthalene analogs **2g** and **2h** were prepared as shown in **Scheme 2**. Employing a similar strategy to **Scheme 1**, commercially available 2-bromo-6-methoxynaphthalene **8a** ( $R^1 = OMe$ ) was coupled to 3-methoxycarbonylphenylboronic acid **5c** ( $R^4 = H$ ,  $R^5 = COOMe$ ,  $R^6 = B(OH)_2$ ), then demethylated, and coupled to the alcohol **7a** ( $R^7 = OH$ ) to give an ester, which upon subsequent hydrolysis provided the carboxylic acid **2g** ( $R^2 = COOH$ ,  $R^3 = H$ ). More efficiently, alkylation of 6-bromo-2-naphthol **8b** ( $R^1 = OH$ ) with chloride **7b**<sup>22</sup> ( $R^7 = Cl$ ), followed by coupling of the resulting aryl ether with 4-carboxyphenylboronic acid **5d** ( $R^4 = COOH$ ,  $R^5 = H$ ,  $R^6 = B(OH)_2$ ) afforded carboxylic acid **2h** ( $R^2 = H$ ,  $R^3 = COOH$ ), directly.



**Scheme 1.** Reagents and conditions: (a) **5a–c**, 2 M  $Na_2CO_3$ ,  $Pd(PPh_3)_4$ , PhMe or DME,  $\uparrow$ , 36–89%; (b)  $BBr_3$ ,  $CH_2Cl_2$ , 0 °C, 32–77% or  $H_2$ , Pd-C, EtOH, EtOAc, rt, 74%; (c) **7a**,  $Ph_3P$  or  $Ph_3P-PS$ , DIAD,  $CH_2Cl_2$  or PhMe, rt, 44–66%; (d) LiOH or NaOH, THF or dioxane, MeOH or EtOH,  $H_2O$ , rt, 18–99%.



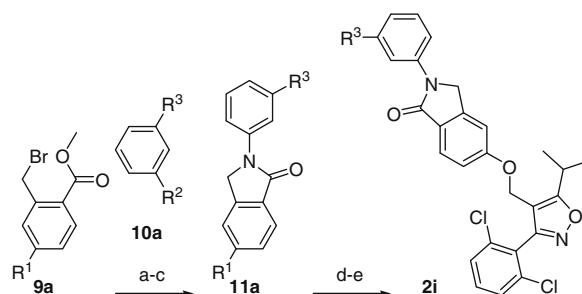
**Scheme 2.** Reagents and conditions: (a) **5c** or **5d**,  $Pd(PPh_3)_4$ , 2 M  $Na_2CO_3$ , PhMe or DME,  $\uparrow$ , 18–36%; (b)  $BBr_3$ ,  $CH_2Cl_2$ , 0 °C, 56%; (c) **7a**,  $PPh_3$ , DIAD,  $CH_2Cl_2$ , 0 °C to rt, 59%; (d) 1 N LiOH, THF, rt, 60%; (e)  $Cs_2CO_3$ , DMF, 65 °C; **7b**, DMF, 59%.

The isoindolin-1-one **2i** was synthesized as illustrated in **Scheme 3**. First, the commercially available methyl 3-aminobenzoate **10a** ( $R^2 = NH_2$ ,  $R^3 = COOMe$ ) was alkylated with the commercially available methyl 2-bromomethyl-4-methoxybenzoate **9a** ( $R^1 = OMe$ ) in the microwave, then the resulting aniline was cyclized to the isoindolin-1-one **11a** ( $R^1 = OMe$ ,  $R^3 = COOMe$ ) under acid catalysis. Lewis acid catalyzed cleavage of the methyl ether led to partial hydrolysis of the methyl ester. The mixture of acid and ester was esterified under Fischer conditions to give the phenol **11a** ( $R^1 = OH$ ,  $R^3 = COOMe$ ). Finally, the previous conditions, for the Mitsunobu coupling and ester hydrolysis, were utilized to provide the carboxylic acid **2i** ( $R^3 = COOH$ ).

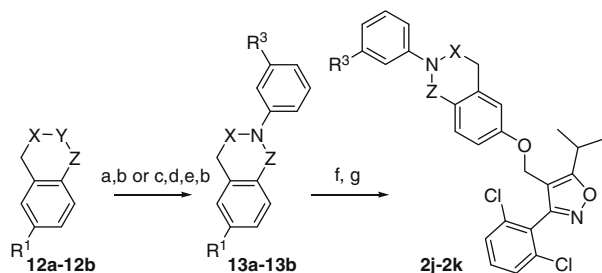
The syntheses of the dihydroisoquinolinones **2j** and **2k** are shown in **Scheme 4**. Copper catalyzed coupling of the commercially available 6-methoxy-3,4-dihydro-2H-isoquinolin-1-one **12a** ( $R^1 = OMe$ ,  $X = CH_2$ ,  $Y = N$ ,  $Z = CO$ ) with the iodide **5a** ( $R^4 = H$ ,  $R^5 = COOEt$ ,  $R^6 = I$ ), followed by methyl ether cleavage and reesterification gave the methyl ester **13a** ( $R^1 = OH$ ,  $R^3 = COOMe$ ,  $X = CH_2$ ,  $Z = CO$ ). Conversely, the methyl ester **13b** ( $R^1 = OH$ ,  $R^3 = COOMe$ ,  $X = CO$ ,  $Z = CH_2$ ) was prepared from the commercially available 6-methoxy-isochroman-3-one **12b** ( $R^1 = OMe$ ,  $X = CO$ ,  $Y = O$ ,  $Z = CH_2$ ). Lactone ring opening, bromination, and esterification with thionyl bromide in methanol, followed by alkylation with aniline **10a** ( $R^2 = NH_2$ ,  $R^3 = COOMe$ ) and acid catalyzed cyclization afforded the methyl ether, which was deprotected to provide the phenol **13b** ( $R^1 = OH$ ,  $R^3 = COOMe$ ,  $X = CO$ ,  $Z = CH_2$ ). The phenols **13a–b** were then alkylated with alcohol **7a** ( $R^7 = OH$ ) under Mitsunobu conditions, followed by hydrolysis of the esters to afford the acids **2j** and **2k**.

The preparation of benzothiazole **2l** is illustrated in **Scheme 5**. The commercially available 2-amino-6-bromobenzothiazole **14a** was coupled to the boronic acid **5c** ( $R^4 = H$ ,  $R^5 = COOMe$ ,  $R^6 = B(OH)_2$ ) via the Suzuki protocol. Then, the aldehyde **7c**, derived from the alcohol **7a** ( $R^7 = OH$ ) by chromium oxidation, was coupled to the aniline nitrogen via reductive amination. Finally, hydrolysis of the methyl ester afforded the carboxylic acid **2l**.

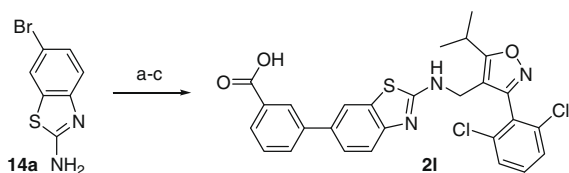
The synthesis of the benzoxazole **2m** is depicted in **Scheme 6**. Suzuki coupling of commercially available 4-bromo-2-nitrophenol



**Scheme 3.** Reagents and conditions: (a) **10a**,  $Et_3N$ , DMF,  $\mu w$ , 150 °C; (b) TFA,  $CH_3CN$ , rt; (c)  $BBr_3$ ,  $CH_2Cl_2$ , 0 °C to rt;  $SOCl_2$ , MeOH,  $\uparrow$ , 24% over three steps; (d) **7a**,  $PPh_3$ , DIAD, rt, 37%; (e) 1 N LiOH, 1,4-dioxane, rt, 72%.



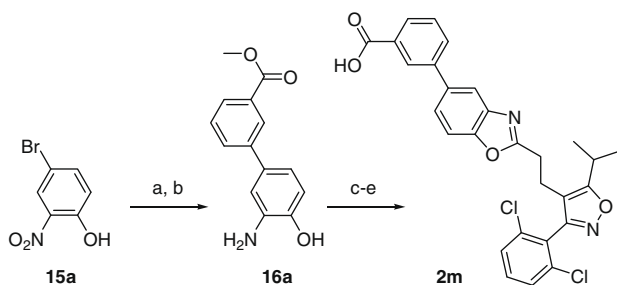
**Scheme 4.** Reagents and conditions: (a) **5a**, CuI, K<sub>2</sub>CO<sub>3</sub>, DMF, 150 °C, 55%; (b) BBr<sub>3</sub>, CH<sub>2</sub>Cl<sub>2</sub>, 0 °C to rt, 68%; SOCl<sub>2</sub>, MeOH, ↓↑, 87%; (c) SOBr<sub>2</sub>, MeOH, PhMe, rt, 90%; (d) **10a**, Et<sub>3</sub>N, PhMe, 90 °C; (e) *p*-TsOH·H<sub>2</sub>O, PhMe, 100 °C; (f) **7a**, PS-PPh<sub>3</sub>, DIAD, CH<sub>2</sub>Cl<sub>2</sub>, rt, 65%; (g) 1 N LiOH, MeOH, THF, μw, 100 °C, 89%.



**Scheme 5.** Reagents and conditions: (a) **5c**, 2 M Na<sub>2</sub>CO<sub>3</sub>, Pd(PPh<sub>3</sub>)<sub>4</sub>, DME, 85 °C, 26%; (b) **7c**, Bu<sub>2</sub>SnCl, Ph<sub>3</sub>SiH, rt to 75 °C, 9%; (c) LiOH, THF, rt, 59%.

**15a** with boronic acid **5c** (R<sup>4</sup> = H, R<sup>5</sup> = COOMe, R<sup>6</sup> = B(OH)<sub>2</sub>), followed by hydrogenation of the nitro group afforded the aniline **16a**. Then, the acid **7d** (R<sup>7</sup> = CH<sub>2</sub>COOH), derived from aldehyde **7c** (R<sup>7</sup> = O) by aldolization with Meldrum's acid and in situ hydrolysis, was activated as the mixed anhydride and coupled to aniline **16a**, followed by acid catalyzed ring closure and ester hydrolysis to give the acid **2m**.

The structure–activity relationships for series **2** (analogs **2a–m**) are shown in Table 1. The benzothienopyridine analogs **2a–d** were all full FXR agonists (%max >80% of GW 4064 **1**) in both the fluorescence resonance energy transfer (FRET) assay for the recruitment of the SRC-1 co-activator peptide to the AF-2 helix of FXR and the transient transfection (TT) assay for the FXR-mediated transcription of a luciferase reporter. The *meta*-substituted carboxylic acid compounds **2a** (TT EC<sub>50</sub> = 32 nM) and **2c** (TT EC<sub>50</sub> = 63 nM) were slightly more potent than the corresponding *para*-carboxylic acid derivatives **2b** (TT EC<sub>50</sub> = 160 nM) and **2d** (TT EC<sub>50</sub> = 220 nM), possibly due to a greater distance separating the negative charge of the carboxylic acid from its positively charged guanidine interaction partner on <sup>331</sup>Arg in the FXR ligand binding domain (LBD) (vide infra). Moreover, **2a** and **2c** are equipotent to the GW 4064 **1** lead (TT EC<sub>50</sub> = 65 nM). Thus, the metabolic liabilities of the stilbene moiety in GW 4064 **1** can be overcome by its replacement



**Scheme 6.** Reagents and conditions: (a) **5c**, Pd(PPh<sub>3</sub>)<sub>4</sub>, DME, 2 M Na<sub>2</sub>CO<sub>3</sub>, 85–95 °C; H<sub>2</sub>SO<sub>4</sub>, MeOH, ↓↑, 14%; (b) Pd/C, H<sub>2</sub>, EtOH, 100%; (c) **7d**, *i*-BuOCOCI, NEt<sub>3</sub>, CH<sub>2</sub>Cl<sub>2</sub>, –5 to –15 °C to rt, 85%; (d) propionic acid, 135–150 °C; (e) 1 N LiOH, THF, rt, 3% over two steps.

**Table 1**  
Activation of human FXR

#	R	FXR FRET EC <sub>50</sub> nM <sup>a</sup> (%max <sup>b</sup> )	FXR TT EC <sub>50</sub> nM <sup>c</sup> (%max <sup>b</sup> )
<b>1</b>		59 (100)	65 (100)
<b>2a</b>		55 (90)	32 (87)
<b>2b</b>		280 (80)	160 (89)
<b>2c</b>		140 (92)	63 (93)
<b>2d</b>		200 (95)	220 (79)
<b>2e</b>		410 (72)	410 (86)
<b>2f</b>		480 (81)	630 (103)
<b>2g</b>		110 (88)	130 (103)
<b>2h</b>		440 (68)	980 (170)
<b>2i</b>		670 (59)	1100 (61)

(continued on next page)

Table 1 (continued)

#	R	FXR FRET EC <sub>50</sub> nM <sup>a</sup> (%max <sup>b</sup> )	FXR TT EC <sub>50</sub> nM <sup>c</sup> (%max <sup>b</sup> )
2j		710 (52)	8300 (112)
2k		1100 (75)	>10,000
2l		960 (91)	380 (123)
2m		1200 (41)	710 (75)

<sup>a</sup> FXR ligand seeking assay measuring ligand-mediated interaction of the SRC-1 peptide (B-CPSSHSSLTERHKILHRLLEQEGSPS-CONH<sub>2</sub>) with the FXR<sup>237-472</sup>LBD, using 5 nM biotinylated FXR LBD coupled to 5 nM allophycocyanin-labeled streptavidin and 10 nM biotinylated SRC-1 coupled to 5 nM Europium-labeled streptavidin as reagents in 10 mM DTT, 0.1 g/L BSA, 50 mM NaF, 50 mM MOPS, 1 mM EDTA, and 50 μM CHAPS, at pH 7.5. The EC<sub>50</sub> values are the mean of at least two assays.

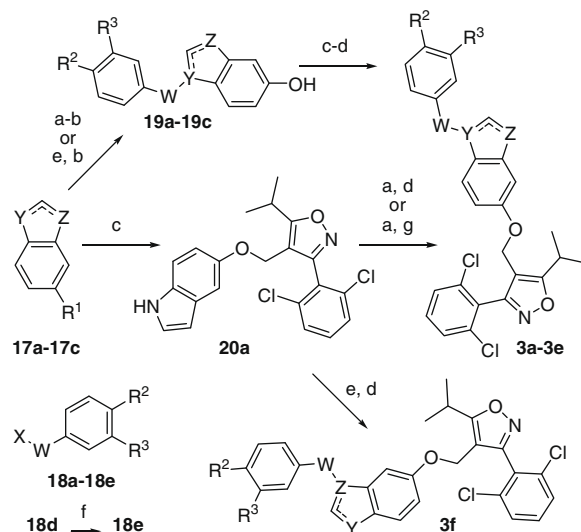
<sup>b</sup> Maximum percent efficacy of the test compound relative to FXR activation via GW 4064 1.

<sup>c</sup> FXR transient transfection assay measuring the ligand-mediated luminescence resulting from FXR-induced transcription of a luciferase reporter. FXR and the luciferase reporter genes are transfected into African green monkey CV-1 kidney cells, then treated with test compound. The EC<sub>50</sub> values are the mean of at least two assays.

with a benzothiazole, with no loss in activity or efficacy. In contrast, the benzothiazole **2e** (TT EC<sub>50</sub> = 410 nM) is less potent than its corresponding benzothiazole **2c**, likely due to the entropic penalty paid to desolvate the nitrogen heteroatom of **2e**, relative to the carbon in **2c**, as it binds into a hydrophobic region of the FXR LBD (vide infra). The reversed benzothiazole **2l** (TT EC<sub>50</sub> = 380 nM) has similar FXR affinity as benzothiazole **2e**. Similarly, the nitrogen containing indole analog **2f** (TT EC<sub>50</sub> = 630 nM) and the nitrogen and oxygen-containing benzoxazole analog **2m** (TT EC<sub>50</sub> = 710 nM) are also less active than the benzothiazole **2c**.

The naphthalene analogs **2g** (TT EC<sub>50</sub> = 130 nM) and **2h** (TT EC<sub>50</sub> = 980 nM) are slightly less potent than the corresponding benzothiazole analogs **2a** and **2b**, with the *para*-derivative **2h** once again being less active than the *meta*-derivative **2g**. Thus, for series **2**, 3-carboxylic acid substitution is optimal. In contrast to the more narrow angle of substituent display by the benzothiazole linker in **2a**, the naphthalene linker in analog **2g** (TT EC<sub>50</sub> = 130 nM) displays its appending groups at ~180°. This may force slight alterations in the FXR LBD, possibly explaining the diminished potency of **2g** relative to **2a**.

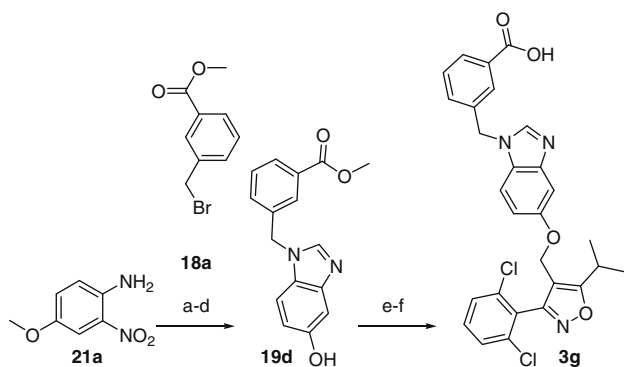
In contrast to the fully aromatic ring system linkers in analogs **2a–h**, the isoindolinone **2i** (TT EC<sub>50</sub> = 1100 nM), and the dihydroisoquinolinones **2j** (TT EC<sub>50</sub> = 8300 nM) and **2k** (TT EC<sub>50</sub> = >10,000 nM) are greater than an order of magnitude less potent than the benzothiazole **2a**. In addition to the higher entropic cost to desolvate the additional heteroatom(s) in these derivatives, the loss of planarity due to partial ring saturation alters the angle of display of the linker ring system substituents, possibly inducing strain in the protein as it accommodates these ligands in the LBD, thus diminishing receptor affinity.



**Scheme 7.** Reagents and conditions: (a) **18a**, **18b**, **18c**, or **18e**, NaH, DMF, 29–99%; (b) H<sub>2</sub>, 10% Pd/C, EtOH, EtOAc, 66–99% or BBr<sub>3</sub>, CH<sub>2</sub>Cl<sub>2</sub>, 0 °C, 65%; (c) **7a**, Ph<sub>3</sub>P or Ph<sub>3</sub>P-PS, DIAD, CH<sub>2</sub>Cl<sub>2</sub>, rt, or **7b**, Cs<sub>2</sub>CO<sub>3</sub>, DMF, 65 °C, 30–71%; (d) LiOH or NaOH, THF or dioxane, MeOH or EtOH, H<sub>2</sub>O, rt or 100 °C, 10–74%; (e) **18a**, (*n*-Bu)<sub>4</sub>Ni, Zn(OTf)<sub>2</sub>, *i*-Pr<sub>2</sub>NEt, PhMe, rt, 53–59%; (f) (COCl)<sub>2</sub>, CH<sub>2</sub>Cl<sub>2</sub>, DMF, 0 °C, 99%; (g) TFA, CH<sub>2</sub>Cl<sub>2</sub>, 0 °C, 50%.

The indole analogs **3a–f** were prepared as shown in **Scheme 7**. Coupling of 5-benzyloxyindole **17a** (R<sup>1</sup> = OCH<sub>2</sub>Ph, Y = NH, Z = CH) to methyl 3-bromomethylbenzoate **18a** (R<sup>2</sup> = H, R<sup>3</sup> = COOMe, W = CH<sub>2</sub>, X = Br), followed by palladium mediated hydrogenolysis of the benzyl ether afforded the phenol **19a** (R<sup>2</sup> = H, R<sup>3</sup> = COOMe, W = CH<sub>2</sub>, Y = N, Z = CH). Alkylation of the phenol **19a** with the chloride **7b** (R<sup>7</sup> = Cl), followed by hydrolysis of the ester provided the indole **3a** (R<sup>2</sup> = H, R<sup>3</sup> = COOH, W = CH<sub>2</sub>, Y = N, Z = CH). Alternatively, the indole **3b** was prepared by alkylation of 5-hydroxyindole **17b** (R<sup>1</sup> = OH, Y = NH, Z = CH) with alcohol **7a** via the Mitsunobu protocol to afford the aryl ether **20a**, which was alkylated with methyl 4-(bromomethyl)benzoate **18b** (R<sup>2</sup> = COOMe, R<sup>3</sup> = H, W = CH<sub>2</sub>, X = Br), followed by hydrolysis of the ester to give the acid **3b** (R<sup>2</sup> = COOH, R<sup>3</sup> = H, W = CH<sub>2</sub>, Y = N, Z = CH). Moreover, the isomeric indole **3c** was prepared from 6-benzyloxyindole **17c** (R<sup>1</sup> = OCH<sub>2</sub>Ph, Y = CH, Z = NH) via Lewis acid promoted alkylation with **18a**, followed by removal of the benzyl protecting group, to afford phenol **19b** (R<sup>2</sup> = H, R<sup>3</sup> = COOMe, W = CH<sub>2</sub>, Y = C, Z = NH). Then, similarly to the synthesis of **3a**, alkylation with **7a** and hydrolysis of the ester gave isomeric indole **3c** (R<sup>2</sup> = H, R<sup>3</sup> = COOH, W = CH<sub>2</sub>, Y = C, Z = NH). The sulfonamide **3d** was prepared by sulfonylation of indole **17a** with the sulfonyl chloride **18c** (R<sup>2</sup> = H, R<sup>3</sup> = COOMe, W = SO<sub>2</sub>, X = Cl), followed by boron tribromide mediated cleavage of the benzyl ether to yield the phenol **19c** (R<sup>2</sup> = H, R<sup>3</sup> = COOMe, W = SO<sub>2</sub>, Y = N, Z = CH). Subsequent alkylation of phenol **19c** with alcohol **7a** and hydrolysis as above afforded acid **3d** (R<sup>2</sup> = H, R<sup>3</sup> = COOH, W = SO<sub>2</sub>, Y = N, Z = CH). Amide **3e** was prepared by acylation of indole **20a** with acid chloride **18e** (R<sup>2</sup> = H, R<sup>3</sup> = COOMe, W = CO, X = Cl), followed by hydrolysis, to give the indole **3e** (R<sup>2</sup> = H, R<sup>3</sup> = COOH, W = CO, Y = N, Z = CH). Acid chloride **18e** was prepared from commercially available acid **18d** (R<sup>2</sup> = H, R<sup>3</sup> = COO*t*-Bu, W = CO, X = OH) employing oxalyl chloride. Finally, Lewis acid promoted alkylation of indole **20a** with bromide **18a**, followed by hydrolysis, gave the 3-substituted indole **3f** (R<sup>2</sup> = H, R<sup>3</sup> = COOH, W = CH<sub>2</sub>, Y = NH, Z = C).

The preparation of benzimidazole analog **3g** is depicted in **Scheme 8**. First, alkylation of aniline **21a** with bromide **18a**, then reduction of the nitro group afforded an *ortho*-dianiline. This intermediate was converted to a benzimidazole with formic acid and



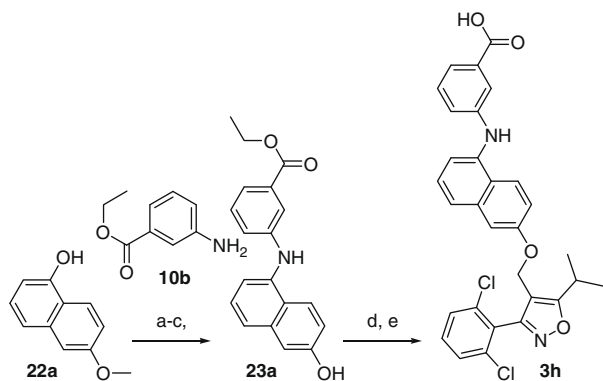
**Scheme 8.** Reagents and conditions: (a) **18a**,  $K_2CO_3$ , DMF, 110 °C;  $H_2$ , 10% Pd/C, EtOH, rt, 21%; (b)  $SnCl_2 \cdot 2H_2O$ , EtOH, reflux, 92%; (c) HCOOH, rt, 86%; (d)  $BBr_3$ ,  $CH_2Cl_2$ , 0 °C; MeOH,  $H_2SO_4$ , reflux, 42%; (e) **7a**,  $PPh_3$ , DIAD,  $CH_2Cl_2$ , 0 °C to rt; (f) 1 N LiOH, 1,4-dioxane, rt, 25%.

the methyl ether was cleaved to provide the phenol **19d**. Mitsunobu coupling of **19d** with the alcohol **7a** and basic hydrolysis of the ester yielded the acid **3g**.

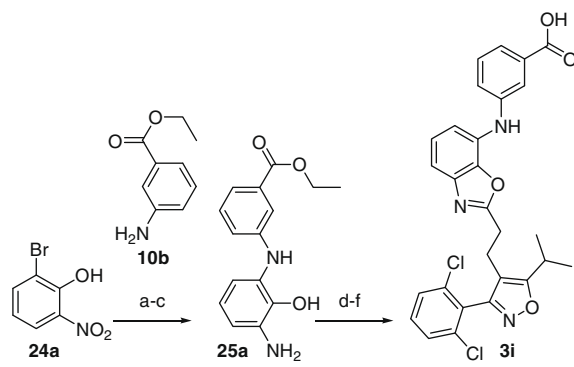
As illustrated in Scheme 9, the naphthalene analog **3h** was prepared from the naphthol **22a**. First, activation of the hydroxy group as the triflate, then Hartwig–Buchwald coupling with the aniline **10b** and boron tribromide mediated hydrolysis of the methyl ether gave the phenol **23a**. Then, O-alkylation of the aniline phenol **23a** with alcohol **7a** via the Mitsunobu protocol provided the ester, which was hydrolyzed to yield the acid **3h**.

The synthesis of the benzoxazole analog **3i** is shown in Scheme 10. Starting from the commercially available bromide **24a**, protection of the phenol as the benzyl ether, then Hartwig–Buchwald coupling with the aniline **10b**, followed by palladium catalyzed reduction of the nitro substituent with concomitant cleavage of the benzyl ether afforded the aniline phenol **25a**. Then, coupling of the acid **7d** with the aniline **25a** provide an amide, which was cyclized to the benzoxazole via acid catalysis. Finally, base-promoted hydrolysis of the ethyl ester yielded the acid **3i**.

The structure–activity relationships for series **3** (analogs **3a–i**) are shown in Table 2. For series **3**, none of the analogs were more potent than the original lead GW 4064 **1**. The *meta*- and *para*-carboxy-phenylmethyl-indole analogs **3a** (TT  $EC_{50}$  = 210 nM) and **3b** (TT  $EC_{50}$  = 330 nM) were slightly less potent FXR agonists than GW 4064 **1**, while the regioisomeric indole analog **3c** (TT  $EC_{50}$  = 930 nM, %max = 32) and benzimidazole **3g** (TT  $EC_{50}$  = 5000 nM, %max = 40) were at least an order of magnitude less active and partial agonists as well. The decreased potency of these analogs is possibly due to less optimal fit of the indole spacer in the FXR

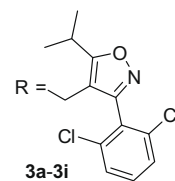


**Scheme 9.** Reagents and conditions: (a)  $Tf_2O$ , pyridine,  $CH_2Cl_2$ , 0 °C, 81%; (b) **10b**,  $Pd_2(dba)_3$ , BINAP, 2 M  $CS_2CO_3$ , PhMe,  $\uparrow$ , 70%; (c)  $BBr_3$ ,  $CH_2Cl_2$ , 0 °C to rt, 35%; (d) **7a**,  $Ph_3P$ , DIAD,  $CH_2Cl_2$ , rt, 37%; (e) LiOH, THF,  $H_2O$ , rt to 60 °C, 54%.



**Scheme 10.** Reagents and conditions: (a) benzyl bromide,  $K_2CO_3$ ,  $CH_3CN$ , 70 °C, 94%; (b) **10b**,  $Pd_2(dba)_3$ , BINAP,  $CS_2CO_3$ , toluene, 100 °C; (c)  $H_2$ , 10% Pd/C, EtOH; (d) **7d**, DCC, HOBT,  $CH_3CN$ , rt; (e)  $CH_3CH_2COOH$ , 130–150 °C, 7.4% over three steps; (f) 1 N LiOH, THF, rt to 60 °C, 57%.

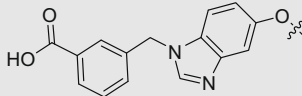
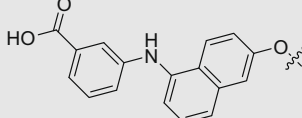
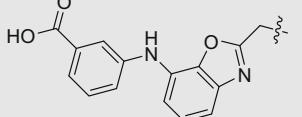
**Table 2**  
Activation of human FXR



#	R	FXR FRET $EC_{50}$ nM <sup>a</sup> (%max <sup>b</sup> )	FXR TT $EC_{50}$ nM <sup>c</sup> (%max <sup>b</sup> )
<b>1</b>		59 (100)	65 (100)
<b>3a</b>		320 (80)	210 (84)
<b>3b</b>		160 (80)	330 (79)
<b>3c</b>		590 (81)	930 (32)
<b>3d</b>		160 (87)	1300 (63)
<b>3e</b>		150 (68)	860 (63)
<b>3f</b>		1500 (25)	>10,000

(continued on next page)

Table 2 (continued)

#	R	FXR FRET EC <sub>50</sub> nM <sup>a</sup> (%max <sup>b</sup> )	FXR TT EC <sub>50</sub> nM <sup>c</sup> (%max <sup>b</sup> )
3g		1400 (38)	5000 (40)
3h		320 (95)	81 (57)
3i		1700 (19)	>10,000

<sup>a</sup> FXR ligand seeking assay measuring ligand-mediated interaction of the SRC-1 peptide (B-CPSSHSLTERHKILHRLLOEGSPS-CONH<sub>2</sub>) with the FXR<sup>237-472</sup>LBD, using 5 nM biotinylated FXR LBD coupled to 5 nM allophycocyanin-labeled streptavidin and 10 nM biotinylated SRC-1 coupled to 5 nM Europium-labeled streptavidin as reagents in 10 mM DTT, 0.1 g/L BSA, 50 mM NaF, 50 mM MOPS, 1 mM EDTA, and 50 μM CHAPS, at pH 7.5. The EC<sub>50</sub> values are the mean of at least two assays.

<sup>b</sup> Maximum percent efficacy of the test compound relative to FXR activation via GW 4064 1.

<sup>c</sup> FXR transient transfection assay measuring the ligand-mediated luminescence resulting from FXR-induced transcription of a luciferase reporter. FXR and the luciferase reporter genes are transfected into African green monkey CV-1 kidney cells, then treated with test compound. The EC<sub>50</sub> values are the mean of at least two assays.

LBD (vide infra). In addition, the larger desolvation penalties to remove water from the indole NH of **3c** and extra nitrogen of benzimidazole **3g** relative to indole **3a**, likely explain the further loss in activity. Indole analogs **3d** (TT EC<sub>50</sub> = 1300 nM) and **3e** (TT EC<sub>50</sub> = 860 nM), where the methylene connector of **3a** is replaced by a sulfonamide or amide linker, were also less potent and efficacious than **3a**, further supporting the desolvation cost hypothesis for the spacer region.

The 3,5-disubstituted indole **3f** (TT EC<sub>50</sub> = >10,000 nM) and the 2,7-disubstituted benzoxazole **3i** (TT EC<sub>50</sub> = >10,000 nM) display their carboxylic acid and isoxazole moieties at narrower angles than the 1,5- and 3,6-disubstituted analogs like **3a** and **3c**, respectively, and are poor FXR agonists. In contrast, naphthalene **3h** (TT EC<sub>50</sub> = 81 nM, %max = 57) places its substituents in similar environments as indole **3a** and is nearly as potent as the starting lead **1**, although it is a partial agonist.

X-ray co-crystal structures of benzothiophene **2c** and indole **3a** with human FXR are shown in Figures 1 and 2, respectively. In Figure 1, the 2.6 Å X-ray co-crystal structure of benzothiophene **2c** is overlaid with the structure of GW 4064 1. The two compounds fit very similarly into the ligand binding domain of the receptor, which may account for the similar potency of the two compounds. In both structures, the two oxygen atoms of the carboxylic acid coordinate to the terminal NH<sub>2</sub> and ε-NH of the guanidine group of <sup>331</sup>Arg (One oxygen atom of the carboxylic acid **2c** is 3.1 Å from the NH<sub>2</sub> nitrogen of <sup>331</sup>Arg, while the other oxygen atom is 2.9 Å from the NH<sub>2</sub> nitrogen of <sup>331</sup>Arg and 2.8 Å from the ε-NH nitrogen of <sup>331</sup>Arg). Also, the carboxylic acids are planar with the aromatic rings, which are in turn, planar with the stilbene (GW 4064 1) and benzothiophene ring **2c**. Moreover, the isoxazole ring of the two compounds form edge to face stacking interactions with <sup>454</sup>Trp located on helix 12. The chlorine atoms of the 3-phenylisoxazole force the phenyl ring to twist out of plane relative to the isoxazole ring. This conformation places the aromatic ring between <sup>328</sup>Met and <sup>365</sup>Met on helices 5 and 7, respectively.

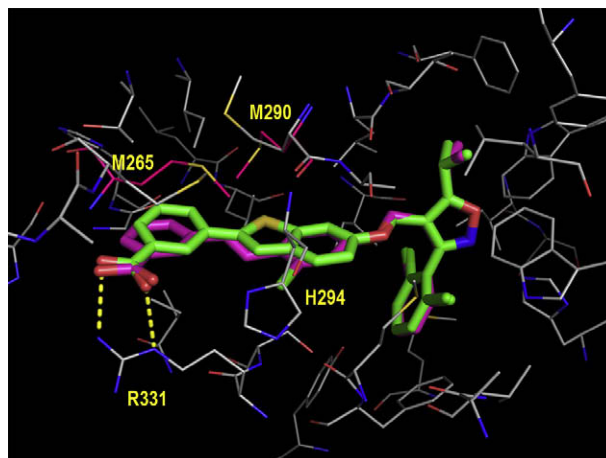


**Figure 1.** Superimposed ligand binding domains of the X-ray co-crystal structures of agonist **2c** (ligand **2c** carbons colored green) and GW 4064 1 (ligand **1** carbons colored magenta) complexed with FXR. The FXR carbons from the co-crystal structure with agonist **2c** are colored gray, with the FXR 'shifted' residues from the co-crystal structure with GW4064 1 colored magenta. The hydrogen bonds are depicted as yellow dashed lines. The coordinates have been deposited in the Brookhaven Protein Data Bank (**1** PDB code 3DC1, **2c** PDB code 3HC5). This figure was generated using PYMOL version 1.0 (Delano Scientific, [www.pymol.org](http://www.pymol.org)).

In Figure 2, the 3.2 Å X-ray co-crystal structure of indole **3a** is overlaid with benzothiophene **2c**. The 3-phenylisoxazole rings of the two compounds fit into the ligand binding domain in a very similar manner. However, in other respects, these two compounds bind to the receptor in distinctly different ways. For example, as noted above, the oxygen atoms of the benzothiophene carboxylic acid coordinate with the terminal NH<sub>2</sub> and ε-NH of the guanidine group of <sup>331</sup>Arg. In contrast, one oxygen atom of the carboxylic acid of indole **3a** forms both of these interactions while the second oxygen atom coordinates with the proximal nitrogen of the imidazole of <sup>294</sup>His (One oxygen atom of the carboxylic acid **3a** is 2.6 Å from the NH<sub>2</sub> nitrogen of <sup>331</sup>Arg, and 2.9 Å from the ε-NH nitrogen of <sup>331</sup>Arg, while the other oxygen atom is 3.2 Å from the nitrogen of <sup>294</sup>His). The additional electrostatic interaction with <sup>294</sup>His forces the carboxylic acid of indole **3a** out of the plane of the ring. Another

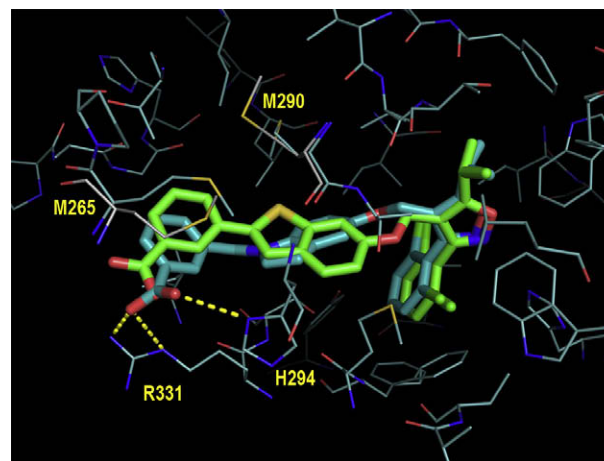


**Figure 2.** Superimposed ligand binding domains of the X-ray co-crystal structures of agonist **2c** (ligand **2c** carbons colored green) and agonist **3a** (ligand **3a** carbons colored cyan) complexed with FXR. The FXR carbons from the co-crystal structure with agonist **2c** are colored gray, with the FXR 'shifted' residues from the co-crystal structure with agonist **3a** colored cyan. The hydrogen bonds are depicted as yellow dashed lines. The coordinates have been deposited in the Brookhaven Protein Data Bank (**2c** PDB code 3HC5, **3a** PDB code 3HC6). This figure was generated using PYMOL version 1.0 (Delano Scientific, [www.pymol.org](http://www.pymol.org)).

**Table 3**  
Pharmacokinetics of FXR agonists in rats

# <sup>a</sup>	$t_{1/2}$ <sup>b</sup> min	$C_l$ <sup>c</sup> (mL/min/kg)	$V_{SS}$ <sup>d</sup> (mL/kg)	$F^e$ (%)
<b>2a</b>	15	66	720	8.5
<b>3a</b>	45	6.7	70	12
<b>3g</b>	31	4.4	85	26

<sup>a</sup> Rats were dosed at 1 mg/kg (iv) and 5 mg/kg (po).

<sup>b</sup>  $t_{1/2}$  is the iv terminal half-life dosed as a solution. All in vivo pharmacokinetic values are the mean of two experiments.

<sup>c</sup>  $C_l$  is the iv total clearance.

<sup>d</sup>  $V_{SS}$  is the iv steady state volume of distribution.

<sup>e</sup>  $F$  is the oral bioavailability.

difference in the binding modes of these two compounds is the spatial relationship between the benzoic acid ring and the adjoining benzothiophene ring of **2c** and indole ring of **3a**. In the case of benzothiophene analog **2c**, these rings are co-planar, while in the crystal structure of indole **3a**, not only are the benzoic acid and indole rings out of plane, but the indole ring is also forced deeper into the pocket. The greater potency of benzothiophene **2c** relative to indole **3a** indicates that a co-planar ligand may more effectively stabilize the active protein conformer, wherein co-repressors are shed and co-activators are recruited, thereby promoting gene transcription. Alternatively, although indole **3a** is non-planar, the ligand causes little perturbation of the FXR ligand binding pocket, yet its active site conformation, to achieve optimal interactions between its carboxylic acid and <sup>331</sup>Arg and <sup>294</sup>His of the FXR ligand binding pocket, is of higher energy than its bulk solution conformation. This free energy cost could account for its lower potency relative to **2c**, as well as the reduced activity of all series **3** analogs.

Several compounds from series **2** and **3** were evaluated in pharmacokinetic studies in rats. As shown in Table 3, benzothiophene **2a** had a very high clearance ( $C_l = 66$  mL/min/kg), which was similar to the hepatic blood flow in the rat. The high clearance of this compound, in conjunction with a low volume of distribution ( $V_{SS} = 720$  mL/kg), resulted in a very short half-life ( $t_{1/2} = 15$  min). The benzothiophene **2a** was also poorly bioavailable ( $F = 8.5\%$ ). Indole **3a** had a significantly lower clearance ( $C_l = 6.7$  mL/min/kg) than the benzothiophene **2a**, however, the resulting improvement in terminal half-life ( $t_{1/2} = 45$  min) was modest due to a very low volume of distribution ( $V_{SS} = 70$  mL/kg). The oral bioavailability ( $F = 12\%$ ) of the indole **3a** was low and only slightly better than that of the benzothiophene. The poor bioavailability of **2a** and **3a** may have been due, in part, to their poor aqueous solubility. In an attempt to improve solubility, a second nitrogen atom was incorporated into the indole ring of **3a** to give the benzimidazole **3g**. This change resulted in a twofold improvement in bioavailability ( $F = 26\%$ ) with little alteration of clearance or terminal half-life. Although the terminal half-lives of these analogs did not improve relative to GW 4064 **1**, the increased oral bioavailability of **3g** suggests that absorption of GW 4064 analogs may be dissolution limited and could be increased by solubility enhancing formulations.

In summary, two series of conformationally constrained analogs of GW 4064 **1** were prepared. Benzothiophene analogs **2a** and **2c** and naphthalene **2g** were potent, full FXR agonists from the more highly constrained series **2**. An X-ray co-crystal structure of benzothiophene **2c** indicates that it binds to the FXR receptor in a man-

ner very similar to GW 4064 **1**. None of the compounds in series **3** were more potent than GW 4064 **1**.

## Supplementary data

Supplementary data associated with this article can be found, in the online version, at doi:10.1016/j.bmcl.2009.06.062.

## References and notes

- Forman, B. M.; Goode, E.; Chen, J.; Oro, A. E.; Bradley, D. J.; Perlmann, T.; Noonan, D. J.; Burka, L. T.; McMorris, T.; Lamph, W. W.; Evans, R. M.; Weinberger, C. *Cell* **1995**, *81*, 687.
- Higashiyama, H.; Kinoshita, M.; Asano, S. *Acta Histochem.* **2008**, *110*, 86.
- Rizzo, G.; Renga, B.; Mencarelli, A.; Pellicciari, R.; Fiorucci, S. *Curr. Drug Targets: Immune, Endocrinol. Metab. Disord.* **2005**, *5*, 289.
- Sinal, C. J.; Tohkin, M.; Miyata, M.; Ward, J. M.; Lambert, G.; Gonzalez, F. J. *Cell* **2000**, *102*, 731.
- Cariou, B.; van Harmelen, K.; Duran-Sandoval, D.; van Dijk, T.; Grefhorst, A.; Bouchaert, E.; Fruchart, J.-C.; Gonzalez, F. J.; Kuipers, F.; Staels, B. *FEBS Lett.* **2005**, *579*, 4076.
- Ma, K.; Saha, P. K.; Chan, L.; Moore, D. D. *J. Clin. Invest.* **2006**, *116*, 1102.
- Zhang, Y.; Lee, F. Y.; Barrera, G.; Lee, H.; Vales, C.; Gonzalez, F. J.; Willson, T. M.; Edwards, P. A. *Proc. Natl. Acad. Sci. U.S.A.* **2006**, *103*, 1006.
- Lambert, G.; Amar, M. J. A.; Guo, G.; Brewer, H. B., Jr.; Gonzalez, F. J.; Sinal, C. J. *J. Biol. Chem.* **2003**, *278*, 2563.
- Maloney, P. R.; Parks, D. J.; Haffner, C. D.; Fivush, A. M.; Chandra, G.; Plunket, K. D.; Creech, K. L.; Moore, L. B.; Wilson, J. G.; Lewis, M. C.; Jones, S. A.; Willson, T. M. *J. Med. Chem.* **2000**, *43*, 2971.
- Watanabe, M.; Houten, S. M.; Wang, L.; Moschetta, A.; Mangelsdorf, D. J.; Heyman, R. A.; Moore, D. D.; Auwerx, J. J. *Clin. Invest.* **2004**, *113*, 1408.
- Inagaki, T.; Choi, M.; Moschetta, A.; Peng, L.; Cummins, C. L.; McDonald, J. G.; Luo, G.; Jones, S. A.; Goodwin, B.; Richardson, J. A.; Gerard, R. D.; Repa, J. J.; Mangelsdorf, D. J.; Kliewer, S. A. *Cell Metab.* **2005**, *2*, 217.
- Inagaki, T.; Moschetta, A.; Lee, Y.-K.; Peng, L.; Zhao, G.; Downes, M.; Yu, R. T.; Shelton, J. M.; Richardson, J. A.; Repa, J. J.; Mangelsdorf, D. J.; Kliewer, S. A. *Proc. Natl. Acad. Sci. U.S.A.* **2006**, *103*, 3920.
- Jung, D.; Inagaki, T.; Gerard, R. D.; Dawson, P. A.; Kliewer, S. A.; Mangelsdorf, D. J.; Moschetta, A. *J. Lipid Res.* **2007**, *48*, 2693.
- Fiorucci, S.; Clerici, C.; Antonelli, E.; Orlandi, S.; Goodwin, B.; Sadeghpour, B. M.; Sabatino, G.; Russo, G.; Castellani, D.; Willson, T. M.; Pruzanski, M.; Pellicciari, R.; Morelli, A. *J. Pharmacol. Exp. Ther.* **2005**, *313*, 604.
- Liu, Y.; Binz, J.; Numerick, M. J.; Dennis, S.; Luo, G.; Desai, B.; MacKenzie, K. I.; Mansfield, T. A.; Kliewer, S. A.; Goodwin, B.; Jones, S. A. *J. Clin. Invest.* **2003**, *112*, 1678.
- Stedman, C.; Liddle, C.; Coulter, S.; Sonoda, J.; Alvarez, J. G.; Evans, R. M.; Downes, M. *Proc. Natl. Acad. Sci. U.S.A.* **2006**, *103*, 11323.
- Fiorucci, S.; Antonelli, E.; Rizzo, G.; Renga, B.; Mencarelli, A.; Riccardi, L.; Orlandi, S.; Pellicciari, R.; Morelli, A. *Gastroenterology* **2004**, *127*, 1497.
- Fiorucci, S.; Rizzo, G.; Antonelli, E.; Renga, B.; Mencarelli, A.; Riccardi, L.; Morelli, A.; Pruzanski, M.; Pellicciari, R. *J. Pharmacol. Exp. Ther.* **2005**, *315*, 58.
- Fiorucci, S.; Rizzo, G.; Antonelli, E.; Renga, B.; Mencarelli, A.; Riccardi, L.; Orlandi, S.; Pruzanski, M.; Morelli, A.; Pellicciari, R. *J. Pharmacol. Exp. Ther.* **2005**, *314*, 584.
- Hanniman, E. A.; Lambert, G.; McCarthy, T. C.; Sinal, C. J. *J. Lipid Res.* **2005**, *46*, 2595.
- Zhang, Y.; Wang, X.; Vales, C.; Lee, F. Y.; Lee, H.; Lusis, A. J.; Edwards, P. A. *Arterioscler., Thromb., Vasc. Biol.* **2006**, *26*, 2316.
- Akwabi-Ameyaw, A.; Bass, J. Y.; Caldwell, R. D.; Caravella, J. A.; Chen, L.; Creech, K. L.; Deaton, D. N.; Jones, S. A.; Kaldor, I.; Liu, Y.; Madauss, K. P.; Marr, H. B.; McFadyen, R. B.; Miller, A. B.; Navas, F., III; Parks, D. J.; Spearing, P. K.; Todd, D.; Williams, S. P.; Wisely, G. B. *Bioorg. Med. Chem. Lett.* **2008**, *18*, 4339.
- Bass, J. Y.; Caldwell, R. D.; Caravella, J. A.; Chen, L.; Creech, K. L.; Deaton, D. N.; Madauss, K. P.; Marr, H. B.; McFadyen, R. B.; Miller, A. B.; Parks, D. J.; Todd, D.; Williams, S. P.; Wisely, G. B. *Bioorg. Med. Chem. Lett.* **2009**, *19*, 2969.
- Kuo, C. H.; Hook, J. B.; Bernstein, J. *Toxicology* **1981**, *22*, 149.
- Sugihara, K.; Kitamura, S.; Sanoh, S.; Ohta, S.; Fujimoto, N.; Maruyama, S.; Ito, A. *Toxicol. Appl. Pharmacol.* **2000**, *167*, 46.
- Akwabi-Ameyaw, A. A.; Deaton, D. N.; McFadyen, R. B.; Navas, F., III. *PCT Int. Appl. WO 005998*, 2009; *Chem. Abstr.* **2009**, *150*, 121632.